Micelles of Star Block $(PSPI)_8$ and PSPI Diblock Copolymers (PS = Polystyrene, PI = Polyisoprene): Structure and Kinetics of Micellization

Grigoris Mountrichas,[†,‡] Maria Mpiri,[†] and Stergios Pispas*[,†,‡]

Department of Chemistry, University of Athens, Panepistimiopolis Zografou, 15771 Athens, and Theoretical and Physical Chemistry Institute, National Hellenic Research Foundation, Vass. Constantinou Avenue, 11635 Athens, Greece

Received October 7, 2004; Revised Manuscript Received December 1, 2004

ABSTRACT: The micellization properties of two star block copolymers, of the type $(PSPI)_8$, where PS = polystyrene and PI = polyisoprene, with PI inner blocks, were investigated, in dilute solutions in two selective solvents for the PS block, namely, dimethylacetamide (DMA) and ethyl acetate (EA), by means of static and dynamic light scattering and viscometry. For comparison purposes the linear diblock arms of the star copolymers, as well as a linear diblock with composition and molecular weight similar to those of one of the stars, were also studied. The carefully designed set of copolymers, as well as the different solvent selectivity toward the two blocks, allowed the elucidation of differences in behavior concerning both the structure of the micelles formed and the kinetics of the micellization process. In DMA the star block copolymers were found to form micelles of smaller size, having lower aggregation number and shorter coronas compared to the diblock case. In comparison with the diblock arm case, star block copolymers formed micelles of essentially the same structure. Star and linear copolymers of low molecular weight formed unimolecular micelles in EA, whereas multimolecular micelles were observed for the higher molecular weight star and linear copolymers. Micelle−unimer equilibrium could be shifted to either side by changes in temperature. Kinetics of micelle formation in EA were faster for the star block case.

Introduction

The behavior of the block copolymers is an interesting field in polymer science, especially due to their ability to self-assemble when they are dissolved in a selective solvent,[1] i.e., a solvent that is good for one of the blocks but poor or precipitant for the other. The macromolecular association has been studied for more than 35 years[2] because of the application potential of this phenomenon in drug delivery, in microreactor applications, or in manipulating the properties of a solid polymeric product.[3] The main parameters that characterize a micellar system are the aggregation number and micellar size and shape. The aforementioned parameters can be influenced by the molecular characteristics of the polymer (overall molecular weight of the copolymer and of each block, composition, architecture), solvent quality (i.e., how selective is the solvent), polymer concentration, and temperature of the solution. The kinetics of micelle formation has received less attention.[4−6]

So far, the majority of the studied micellar systems consist of linear diblock[1,7−13] and triblock[14−18] copolymers. In the past few years, due to the developments in the field of polymer synthesis, the effect of polymer architecture in the fundamental micellization properties of complex macromolecules has started to be investigated.[19−35]

In this paper, we report results on the micellization properties of two carefully synthesized star block copolymers, of the type (polystyrene-*b*-polyisoprene)$_8$, $(PSPI)_8$, where PI is the inner block, having different molecular weights and similar compositions (Scheme 1). These results are compared with data on two linear diblocks, the arms of these stars, and a linear diblock which has almost the same molecular weight and composition as one of the stars. Our primary goal is to investigate the influence of the architecture, topology, and molecular weight of this type of copolymer on its micellization properties, i.e., the structure of the micelles formed in this case and also the kinetics of micelle formation where possible. The data are collected from static light scattering, dynamic light scattering, and viscometry experiments in dilute solutions of two solvents with different selectivities for the block of polystyrene, dimethylacetamide (DMA), and ethyl acetate (EA). The solubility parameters values,[36] δ, for the above solvents, as well for the blocks of styrene and isoprene, are, for PS, $\delta = 17.5$ MPa$^{1/2}$, for PI, $\delta = 15.8$ MPa$^{1/2}$, for DMA, $\delta = 22.1$ MPa$^{1/2}$, and, for EA, $\delta = 18.6$ MPa$^{1/2}$.

Scheme 1. Formation of Micelles by a Star Block Copolymer (Top) and a Linear Block Copolymer (Bottom)

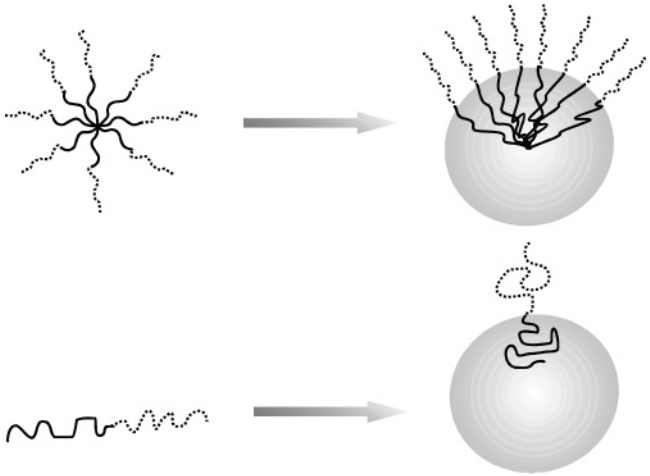

[†] University of Athens.
[‡] National Hellenic Research Foundation.

10.1021/ma047937v CCC: $30.25
Published on Web 01/14/2005

Table 1. Molecular Characteristics of the Samples Studied

sample	M_w[a] ($\times 10^{-4}$)	$M_{n,ps}$[b] ($\times 10^{-4}$)	[PS][c] (wt %)	M_w/M_n[d]	f	R_h[e] (nm)	A_2 (mL mol g^{-2}) ($\times 10^4$)
8-80/50	62.0	4.40	54	1.06	7.7	22.7	3.52
80/50	8.07	4.40	54	1.02	1	11.1	9.12
8-40/50	31.3	2.19	55	1.06	7.9	14.9	4.58
40/50	3.98	2.19	55	1.04	1	7.2	11.7
600/50	67.8	34[a]	51	1.08	1	23.1	4.7

[a] LALLS in THF at 25 °C. [b] Membrane osmometry in toluene at 37 °C. [c] NMR in $CHCl_3$ at 30 °C. [d] SEC in THF at 30 °C. [e] DLS in THF at 25 °C.

According to the above values, ethyl acetate is more selective (a better solvent) than dimethylacetamide toward PS. On the other hand PI is insoluble in DMA, even at 60 °C, and in EA at room temperature.

Experimental Section

Polymer Synthesis. All samples were synthesized by anionic polymerization high-vacuum techniques,[35] using a chlorosilane having eight outer reactive chlorine atoms as linking agent. The diblock samples were synthesized by sequential polymerization of the two monomers. Initially styrene was polymerized using *sec*-BuLi as initiator, followed by the addition of isoprene and deactivation with degassed methanol. The star-type polymers were prepared by reaction of the living diblock arms (PS-*b*-PI^-Li^+) with the linking agent. The desired $(PSPI)_8$ eight-arm stars, having PI inner blocks, were isolated from the reaction mixture by solvent/nonsolvent fractionation (toluene/methanol). The fractionated final product (pure star block copolymers) were rigorously characterized by size exclusion chromatography, membrane osmometry, low-angle laser light scattering, dynamic light scattering, and ^1H NMR to provide the molecular characteristics of the materials and confirm the high degree of compositional, molecular weight, and architectural homogeneity of the copolymers as well as to determine the structural parameters of the isolated macromolecules. The molecular characteristics of the samples under study are given in Table 1. The code names that have been used in this paper for the samples are composed of three numbers indicating the number of arms (first number; in the case of linear polymers this number is omitted), the molecular weight of the arms in thousands (second number), and, finally, the percentage of the polystyrene in the macromolecule (third number). For example, samples 8-40/50 and 8-80/50 are different only in molecular weight, and 8-80/50 and 600/50 have almost the same molecular weight and composition but different architectures. In this way, conclusions about the influence of architecture are more straightforward, and some understanding of the fundamental laws that govern micelle formation can be gained. Finally, comparison between the stars and their arms (8-40/50 with 40/50 and 8-80/50 with 80/50) indicates the influence of the macromolecular topology on the properties of the micelles.

Solvent Purification and Solution Preparation. Analytical grade DMA was dried over CaH_2 by reflux for 24 h and was fractionally distilled just prior to use. Stock solutions were prepared by dissolving a weighed amount of sample in the appropriate volume of dried solvent. Heating of the stock solution at 60 °C was necessary for complete dissolution of the polymers. All the samples were dissolved in DMA after 24 h, with the exception of 8-80/50 and 600/50, which dissolved after two or more days (the dissolution time depended on the concentration of the solutions, due to their high molecular weight). Stock solutions had the characteristic blue tint related to the presence of micelles. No precipitation was observed from any solution after it was allowed to stand at room temperature for several weeks. By dilution of the stock solutions, solutions of lower concentration were prepared. For the light scattering experiments the solutions were filtered through 0.45 μm nylon filters, whereas for viscosity measurements 1.2 μm nylon filters were used.

In the case of EA the same solution preparation protocol was followed as in the case of DMA. The only difference was the fact that all the samples were dissolved in less than 24 h, when they were heated at 60 °C. This is because ethyl acetate is a better solvent for the polyisoprene block compared to DMA. Additionally, the characteristic blue tint was apparent only in the solutions of 600/50 and 8-80/50 at room temperature, i.e., in the solutions of polymers with the higher molecular weights.

Methods. The static light scattering measurements were performed with a Series 4700 Malvern system composed of a PCS5101 goniometer with a PCS7 stepper motor controller, a Cyonics variable-power Ar^+ laser, operating at 488 nm and with 10 mW power, a PCS8 temperature control unit, and a RR98 pump/filtering unit. Toluene was used as a calibration standard. Additional measurements were also performed with a Chromatix KMX-6 low-angle laser light scattering photometer ($\theta = 6-7°$), equipped with a He−Ne laser operating at $\lambda = 633$ nm. Apparent weight-average molecular weights, $M_{w,app}$, and second virial coefficients, A_2, were determined from the concentration dependence of the reduced scattering intensity by use of the equation

$$Kc/\Delta R_\theta = 1/M_{w,app}P(\theta) + 2A_2c + ... \quad (1)$$

where K is a combination of optical and physical constants, including the differential refractive index increment dn/dc, c is the concentration, ΔR_θ is the difference between the Rayleigh ratio of the solution and the solvent, and $P(\theta)$ is the form factor. Radii of gyration, R_g, where possible, were determined from the angular dependence of the reduced scattering intensity. The dn/dc values required for the light scattering measurements were obtained by a Chromatix KMX-16 laser differential refractometer, operating at 633 nm and calibrated with NaCl solutions, or with a Wyatt Technologies Optilab DSP interferometer operating at 488 nm, in the appropriate solvent and temperature.

Dynamic light scattering experiments were carried out on the same Malvern system operating in the dynamic mode. A 192-channel correlator was used for accumulation of the data. Correlation functions were analyzed by the cumulants method and by the use of the CONTIN software provided by the manufacturer. The scattering intensity was measured at scattering angles between 45° and 135°. Apparent translational diffusion coefficients at zero concentration, $D_{0,app}$, were calculated, after extrapolation to zero angle by the use of eq 2, where D_{app} is the diffusion coefficient measured at each

$$D_{app} = D_{0,app}(1 + k_D c) \quad (2)$$

concentration and k_D is the coefficient at the concentration dependence of D_{app}. Apparent hydrodynamic radii, R_h, were determined by eq 3, where k_B is the Boltzmann constant, T is

$$R_h = k_B T/6\pi\eta_0 D_{0,app} \quad (3)$$

the absolute temperature, and η_0 is the viscosity of the solvent. The light scattering experiments were performed at 25 °C, but we have also studied the influence of the temperature in the formed micelles. The protocol was followed for the study of the temperature dependence included heating of the samples from 25 to 55 °C by a step of 5 °C/15 min, a period after which intensity measurements were constant and were measured. The molecular weight and the diffusion coefficient determined by light scattering are apparent quantities because of the possibility of changes in aggregation number with concentration and because of the different refractive indices of the two blocks.[1,2]

For the viscosity measurements, Cannon-Ubbelohde dilution viscometers were used in a temperature-controlled bath at 25 °C (temperature stability ±0.02 °C). Flow times for the solvent and the solutions were measured with a Scott-Geräte AVS 410

Table 2. Light Scattering and Viscometric Results from DMA Solutions at 25 °C

sample	$M_{w,app}$ ($\times 10^{-6}$)	A_2 (mL mol g^{-2}) ($\times 10^6$)	N_w	$D_{0,app}$ (cm^2/s) ($\times 10^8$)	k_D (mL g^{-1})	R_h (nm)	$[\eta]$ (mL g^{-1})	k_H	$R_{v,app}$ (nm)
8-40/50	5.9	6.0	19	9.6	55.3	25.3	11.62	0.75	22.2
40/50	7.1	7.8	177	9.5	25.6	25.6	12.33	0.89	24.0
8-80/50[a]	27.7	9.7	45	5.1	127.4	48.0	32.23	1.09	52.1
80/50[a]	24.2	0.65	299	5.6	8.5	43.4	14.32	1.52	38.0
600/50[a]	918	1.1	1354	1.3	−46.0	181	36.93	1.70	175

[a] Light scattering measurements give the following R_g values for these samples: 8-80/50, R_g = 30.7 nm; 80/50, R_g = 24.7 nm; 600/50, R_g = 103 nm.

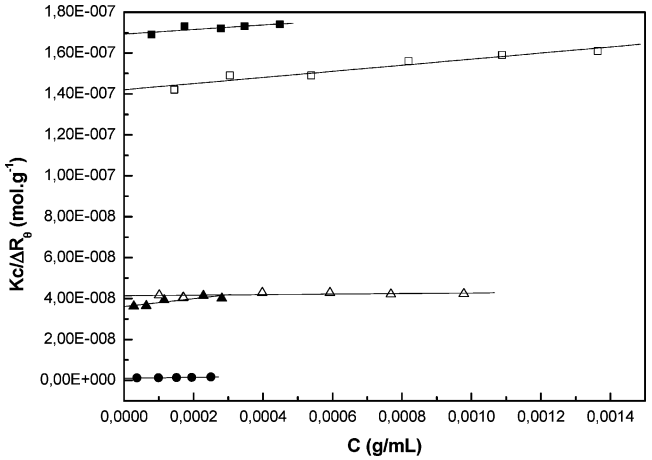

Figure 1. Static light scattering plot for block copolymers in DMA at 25 °C: 8-40/50 (■), 40/50 (□), 8-80/50 (▲), 80/50 (△), 600/50 (●).

automatic flow timer and were always greater than 150 s. Data were analyzed by using the Huggins

$$\eta_{sp}/c = [\eta] + k_H[\eta]^2 c + ... \quad (4)$$

and Kraemer

$$\ln \eta_r/c = [\eta] + k_K[\eta]^2 c + ... \quad (5)$$

equations, where $[\eta]$ is the intrinsic viscosity and k_H and k_K are the Huggins and Kraemer constants, respectively. Finally, the viscometric equivalent sphere radii, R_v, were calculated from eq 6, where $M_{w,app}$ is the weight-average molecular weight determined by light scattering.

$$R_v = (3/10\pi N_A)^{1/3}([\eta]M_{w,app})^{1/3} \quad (6)$$

Results and Discussion

Micellar Properties in DMA. The results from the static light scattering experiments in DMA, a selective solvent for the PS block, are given in Table 2. A representative plot for the concentration dependence of the reduced scattering intensity of all samples in DMA is shown in Figure 1. As can be seen at the concentration range (3×10^{-5} to 10^{-3} g mL^{-1}) used in the experiments the equilibrium is shifted completely in favor of the micelles, where the properties of the solution are dominated by the presence of associates. Presumably, the region of unimer−micelle coexistence is outside the accessible concentration window. The apparent molecular weight, $M_{w,app}$, is very close to the true one because of the high values of dn/dc,[36] for each block and the copolymers in this solvent, the low values of A_2, and the high degree of molecular uniformity. The values of the molecular mass of the associates are obtained from linear extrapolation to infinite dilution. It is obvious that among the polymers with the same architecture the molecular weight increases as the molecular weight of the insoluble branches increases too. Moreover, the micelles that are formed by the star polymers or their arms have almost the same molecular weight, and this indicates that the topology of the chains in the core does not affect this parameter. The values of the second virial coefficient are almost 2 orders of magnitude smaller than the ones determined for the unimers in a good solvent, THF (see Table 1), due to the selectivity of the solvent and the high molecular weight of the micelles. As far as the weight-average aggregation number, defined as

$$N_w = M_{w,micelle}/M_{w,unimers}$$

is concerned, among the samples with the same architecture, an increase in the overall length of the insoluble block causes an increase in this parameter.[8,9] Furthermore, it is noticeable that the star copolymers form micelles which have much smaller aggregation numbers than the ones determined for the micelles formed by their arms. Finally, comparison between 8-80/50 and 600/50, the two copolymers with the same molecular weight and composition but different architectures, indicates that the N_w of the linear copolymer is almost 30 times greater than the respective star copolymer. This is in agreement with the results reported in other works.[19−34] The reason for this behavior must be that the more arms a star polymer possesses the greater the difficulty to accommodate itself in a micelle, due to excluded volume effects as well as to elastic energy loss of the soluble arms.

The results from dynamic light scattering are also given in Table 2, and a representative plot of the concentration dependence of the diffusion coefficient is shown in Figure 2. The diffusion coefficients have very low values due to the low mobility of the supramolecular structure with respect to molecularly dissolved polymers. k_D values show a different trend between the linear copolymers and the star ones. Thus, in the case of linear polymers, k_D decreases as the molecular weight increases, while in the case of star polymers, the opposite behavior is observed. Due to the complex nature of the parameter, which includes thermodynamic and hydrodynamic factors, a clear explanation of the observed behavior is not possible. As far as the hydrodynamic radii, R_h, are concerned the comparison between the star copolymers and their arms shows that there are no noticeable differences in the size of the micelles, indicating that the presence of a junction point in the core of the star copolymer affects neither the mass nor the overall dimensions of the micelles. However, the difference in micellar hydrodynamic radii between samples 8-80/50 and 600/50 is high, although the unimers have almost the same molecular weight and

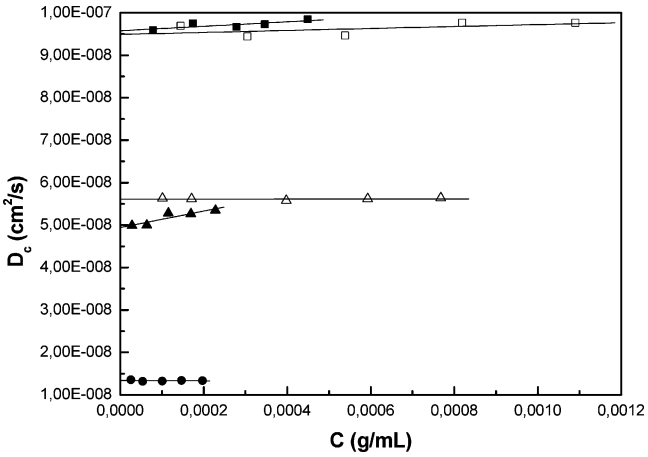

Figure 2. Dynamic light scattering plot for block copolymers in DMA at 25 °C: 8-40/50 (■), 40/50 (□), 8−80/50 (▲), 80/50 (△), 600/50 (●).

composition. This difference is attributed to the "breaking" of PS and PI chains into eight equal parts, in the case of the star polymer, 8-80/50, which has as a result the micelle adopting a structure with much smaller dimensions than those of the micelle which is formed by the respective linear one (Scheme 1). It also has to be mentioned that R_h values are independent of scattering angle, which means that the formed micelles are spherical. Finally, the polydispersity values, expressed by the ratio μ_2/Γ^2 (where μ_2 is the second cumulant and Γ is the decay rate of the correlation function), are less than 0.1, revealing that the micelles formed are almost monodisperse in size.

Dilute solution viscometric results are presented in Table 2. From the experimental findings it is obvious that the intrinsic viscosity values, $[\eta]$, are rather low if one takes into account the high molecular weight of the multimolecular micelles. This is in agreement with the results of R_h from dynamic light scattering. It is also worth mentioning that the values of $[\eta]$ for the samples 8-80/50 and 600/50 are higher in comparison with those of the other samples. The k_H values are larger for the diblocks than for the star blocks. This may indicate a less compact structure for the micelles of the star copolymers due to the steric hindrance of the many arms. Furthermore, the k_H values are large, compared to typical values for polymers in good solvents, due to the increased hydrodynamic interactions within the micelles. In most cases k_H values are close to or higher than the theoretical value for hard spheres ($k_H = 0.99$[38]), indicating the highly compact spherical structure of these micelles. Although it is possible that, in the concentration range (3×10^{-3} to 2×10^{-2} g mL^{-1}) used for the viscometric experiments (much higher than in the case of light scattering experiments), the structure of the supramolecular associates may be changed, the good agreement between R_v and R_h values, within experimental error, shows that structure transformation does not take place at higher concentrations.

By combination of the results obtained by the employed methods and the use of some theoretical or simple mathematical relations, some other structural micellar characteristics could be derived. The results from this procedure are given in Table 3. The first conclusion that can be drawn is that all micelles studied resemble hard spheres, because the values of the ratio R_v/R_h are close to unity (the theoretically calculated value for the hard spheres). This is in agreement with the calculated k_H values and with the results from dynamic light scattering in different angles. Also the ratio R_g/R_h, where available, takes values (0.57−0.64) that are indicative of a spherical structure.

The number of soluble chains per micelle in each case is shown in the second column. For the linear macromolecules this number is identical with the aggregation number, but in the case of star copolymers $N_{PS,corona} = 8N_w$. Between 8-40/50 and 8-80/50 the increase in the molecular weight causes an increase in $N_{PS,corona}$. The effect of architecture is considerable; the energy penalty during the association of 8-80/50, because of its nonlinear architecture, has as a result a decrease of this parameter in comparison with that of the diblock 600/50.

The radius of the micellar core, R_c, can be derived from eq 7, where $M_{w,mic}$ is the apparent weight-average molecular weight of the micelles determined by light scattering, wt_{PI} is the weight fraction of PI in the

$$R_c = (3M_{w,mic}wt_{PI}/4\pi N_A d_{PI}\Phi_{PI})^{1/3} \quad (7)$$

macromolecule, N_A is the Avogadro number, d_{PI} is the density of PI (0.89 g/mL), and Φ_{PI} is the volume fraction of PI in the core of the micelle, which in the case of PI in DMA can be assumed to be equal to 1 (the case of a dry PI core) due to the high selectivity of the solvent. From the data in Table 3, it seems that the increase in the molecular weight in the star copolymers is followed by an increase in R_c. Finally, it is noticeable that the existence or nonexistence of a junction point in the micellar core does not affect the dimensions of the core, as revealed by the comparison of the star-type polymers and their arms.

Another important micellar characteristic is the core/corona interfacial area per molecule, A_c (or per polymer chain, A_c/n), which can be calculated as

$$A_c = 4\pi R_c^2/N_w \quad (8)$$

The values of the core area per polymer chain are obtained by dividing A_c by the number of soluble PS blocks per molecule in each case (Table 3). It is observed that for the micelles formed by the star block copolymers A_c is higher than in the case of linear diblocks, probably due to the existence of eight chains per molecule, whereas at the linear diblock copolymers only one chain exists. More interesting are the experimental results for the core area per chain, A_c/n. The increase of molecular weight causes an increase in this parameter, not only between the samples of star polymers but also among the linear ones. There is also a large difference in A_c/n between 8-80/50 and 600/50. The reasons for this difference must be the existence of a junction point in 8-80/50, which forces the arms to be close together, and the fact that the short PS chains in 8-80/50 can adopt more elongated structures than the longer ones in 600/50.

Since the hydrodynamic radii and the core radius of the micelles have already been determined, the corona thickness, L, could be easily evaluated by subtracting R_c from R_h (Table 3). Comparison between the micelles formed by the two star block copolymers indicates that the increase in molecular weight has as a result a direct increase in this parameter. Moreover, it seems that the architecture plays an important role in the thickness

Table 3. Geometrical Characteristics of the Micelles Formed in DMA

sample	R_v/R_h	$N_{PS,corona}$	R_{core} (nm)	A_c (nm^2)	A_c/n (nm^2)	L (nm)	$\sigma N^{6/5}$	% extension	$L/\langle r_0^2\rangle^{1/2}$
8-40/50	0.88	152	$10._5$	$72._9$	$9._1$	15	4.2	28.1	3.6
40/50	0.94	177	$11._1$	$8._8$	$8._8$	14	4.4	27.3	3.4
8-80/50	1.09	360	$17._7$	$87._5$	$10._9$	30	8.1	28.7	5.2
80/50	0.87	299	$16._9$	$12._0$	$12._0$	27	7.4	25.1	4.6
600/50	0.97	1354	$58._1$	$31._3$	$31._3$	123	32.9	15.1	7.5

of the corona (obviously because of the breaking of a long PS chain in eight shorter chains in the case of 8-80/50 compared to 600/50).

Turning now to the conformation of the PS chains located in the corona, there are some criteria according to which one could estimate the degree of chain elongation. Such a criterion is the quantity $\sigma N^{6/5}$, adopted by Eisenberg et al.[39,40] When this factor takes values greater than 1, the corona chains exhibit a stretched conformation. σ is a dimensionless parameter which describes the chain density at the core/corona[41,42] interface and is given by the following equation:

$$\sigma = \alpha^2/(A_c/n) \tag{9}$$

where α is the length of the repeat unit (0.25 nm for PS) and A_c/n is the core area per soluble chain. Additionally, N is the degree of polymerization of the corona chain. The estimated values of this factor are listed in Table 3 and indicate that the PS chains in every micelle adopt a stretched conformation. Furthermore, an estimation of the degree of chain extension, in relation with the fully extended structure, can be evaluated by eq 10. The results of this parameter show

$$\%\ \text{extension} = 100L/\alpha N \tag{10}$$

that, independent of the molecular weight of the copolymers and the topology of the chains in the core, the percent chain extension is practically the same for all the samples, with the exception of 600/50, for which this parameter takes very low values, presumably due to the large length of this chain. Finally, in the same table we report the ratio of the corona thickness to the unperturbed end-to-end distance for linear PS chains with the same molecular weight with the corresponding blocks of the copolymer in a Θ solvent.[43] It seems that an increase in molecular weight causes an increase in this parameter, among the samples with the same architecture and that the architecture has a large influence on this ratio (compare the values for 8-80/50 and 600/50).

Finally, the behavior of the micelles as a function of temperature was studied. The results of these experiments show that all the micelles are stable in the increase in temperature between 25 and 55 °C, as a result of the high selectivity of the solvent.

Micellar Properties in EA. Judging from the solubility parameter values, EA is a better solvent for the polyisoprene block than DMA, but it is also selective. The immediate result of this fact is that not all the samples form multimolecular micelles when they are dissolved in this solvent, as the results in Table 4 and the representative plot from static light scattering in Figure 3 indicate. Only samples 8-80/50 and 600/50 form multimolecular micelles due to their larger molecular weights. Furthermore, it has been observed, at the initial stages of this investigation, that the properties of the multimolecular micelles are time dependent. Because of this, the results for samples 8-80/50 and 600/50 are given at two times: 24 h after the dissolution of the samples and after three weeks. We believe that the second series of measurements are those of equilibrium, since no change in the micellar properties is observed beyond that period. The solutions of the remaining samples, where the existence of the unimolecular micelles was observed, have also been measured at different times (for a period of a month), but the results indicate that the properties of these solutions are stable over time.

Table 4. Light Scattering Results from Ethyl Acetate Solutions after 24 h, at 25 °C

sample	$M_{w,app}$ ($\times 10^{-6}$)	A_2 (mL mol g^{-2}) ($\times 10^6$)	N_w	$D_{0,app}$ (cm^2/s) ($\times 10^8$)	k_D (mL g^{-1})	R_h (nm)
8-40/50	0.27	52.7	1	46.0	−4.0	11.1
40/50	0.04	40.6	1	109	−9.3	4.7
8-80/50	1.0	−18.0	2	27.0	−27.7	19.0
80/50	0.09	6.76	1	75.8	−20.2	6.8
600/50	83.7	6.68	123	6.1	3.4	84.5

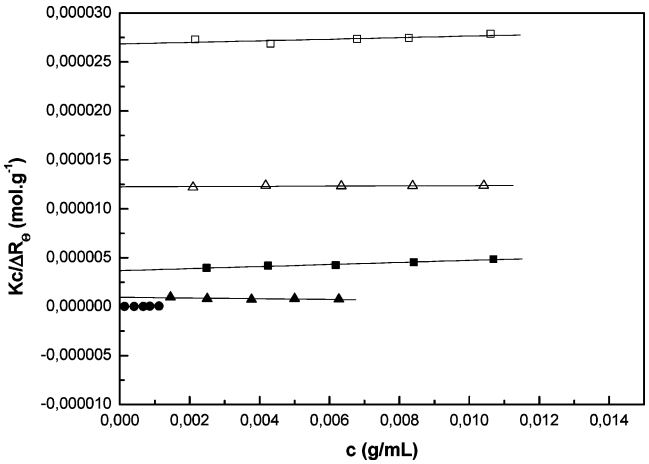

Figure 3. Static light scattering plot for block copolymers in EA at 25 °C: 8-40/50 (■), 40/50 (□), 8−80/50 (▲), 80/50 (△), 600/50 (●).

The static light scattering results of the first series of experiments, 24 h after the dissolution of the samples, show that only samples 8-80/50 and 600/50 form multimolecular micelles; this is because they are the samples having the larger molecular weight of polyisoprene, i.e., the larger insoluble block. For the rest of the samples apparent molecular weight values determined in EA are the same, within experimental error, as those obtained in the nonselective solvent THF.

The results from the static light scattering for the second series of experiments are given in Table 5. This table includes the results for samples 8-80/50 and 600/50, where changes in micellar structure were observed, and additionally the results for sample 8-40/50, where no remarkable change is indicated. The aggregation number for star block copolymer 8-80/50 doubles in a period of three weeks, in agreement with the negative starting A_2. On the contrary, in the case of 600/50, a

Table 5. Light Scattering and Viscometric Results from EA Solutions after Three Weeks, at 25 °C

sample	$M_{w,app}$ ($\times 10^{-6}$)	A_2 (mL mol g^{-2}) ($\times 10^6$)	N_w	$D_{0,app}$ (cm^2/s) ($\times 10^8$)	k_D (mL g^{-1})	R_h (nm)	$[\eta]$ (mL g^{-1})	k_H	$R_{v,app}$ (nm)
8-40/50	0.29	67.2	1	45.8	−3.7	11.2	30.1	0.77	10.9
8-80/50	2.19	0.98	4	19.8	18.2	25.9	36.2	0.76	18.2
600/50[a]	62.5	13.0	92	6.2	17.1	83.3	51.6	1.58	88.1

[a] R_g for this sample is equal to 47.3 nm.

Table 6. Geometrical Characteristics of the Micelles Formed in EA

sample	R_v/R_h	$N_{PS,corona}$	R_{core} (nm)	A_c (nm^2)	A_c/n (nm^2)	L (nm)	$\sigma N^{6/5}$	% extension	$L/\langle r_0^2\rangle^{1/2}$
8-40/50	0.97	8	3.8	184.3	23.0	7.4	1.7	14.1	2.1
8-80/50	0.70	32	7.6	181.4	22.7	18.3	3.9	17.5	3.5
600/50	1.06	92	23.7	76.8	76.8	59.6	13.7	7.2	7.9

large decrease in this parameter is observed during the same time period.

As in the case of DMA, dynamic light scattering experiments have also been performed; the results from the first series of experiments are presented in Table 4. It seems that the unimolecular micelles have very low values of the hydrodynamic radii and that their dimensions are smaller than those obtained in THF, as expected because of the partial collapse of the PI block. On the other hand, samples 8-80/50 and 600/50, which form multimolecular micelles, show greater values for this parameter. Moreover, similar to the results in DMA, the architecture dramatically influences this micellar characteristic. R_h is smaller for the star block copolymer.

The results from the second series of experiments are given in Table 5. The only change in R_h values is indicated for the star block copolymer, 8-80/50. An analogous change was expected in the overall dimensions of sample 600/50, mainly because of the change in the aggregation number, but this is not observed. Presumably, the change in the aggregation number is not large enough to produce a detectable change in the dimensions of the micelles, and this observation must be associated with the spherical shape of the micelles in EA. The spherical shape is confirmed by the fact that practically the same R_h is measured independent of the angle, in DLS experiments.

The viscosity behavior of the samples has also been studied. Due to the limited amount of the sample, only one series of experiments have taken place and only the star block copolymers and the linear one, 600/50, have been studied. These experiments were done after three weeks of the dissolution of the samples. The results are also given in Table 5. It is obvious that the micelles that are formed, unimolecular and multimolecular, are not as compact as in the case of the first solvent, DMA. This is indicated by the intrinsic viscosity values, which are rather high. The lower k_H values in this solvent lead to the same conclusion. This can be a consequence of the larger swellability of the core in EA. Furthermore, as was observed in the case of DMA, the different architectures between 8-80/50 and 600/50 influence their micellar characteristics. In Table 6 some additional micellar characteristics for the two star-type copolymers, 8-40/50 and 8-80/50, and also for the linear one, 600/50, are given. These characteristics were derived using the same procedure as in the case of DMA and for the systems after the three week period. The general conclusion is that the basic micellar characteristics show the same trend as in the case of DMA. It is interesting to note that even in the case of unimolecular micelles of sample 8-40/50 some extension of the soluble PS chain is observed.

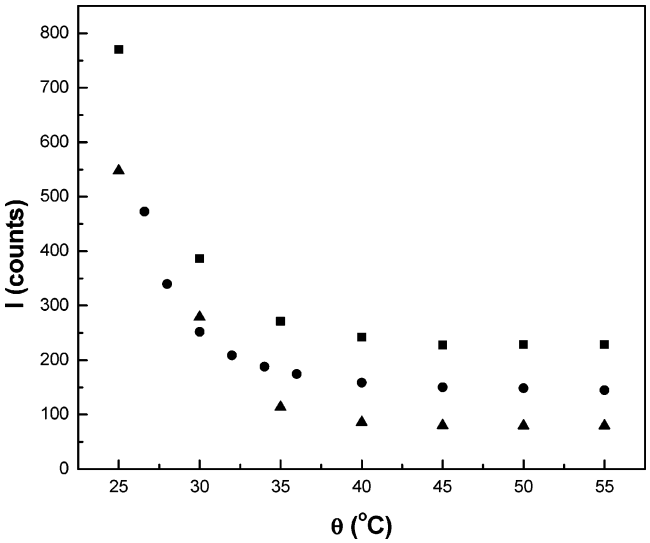

Figure 4. Light scattering intensity vs temperature, in EA, for sample 8-80/50: 1×10^{-3} g/mL (▲), 4×10^{-3} g/mL (●), 6×10^{-3} g/mL (■).

The influence of temperature on the formed multimolecular micelles has been investigated in more detail in EA. Here the results are more interesting than in the DMA because it was possible to determine the critical micelle temperature in the range from 25 to 55 °C. Figures 4 and 5 show how the intensity decreases with the increase in temperature for samples 8-80/50 and 600/50 (the hydrodynamic radii of the micelles show similar behavior). For sample 8-80/50, the critical micellization temperature, cmt, is at about 32 °C and it is nearly independent of the solution concentration, in the concentration range studied. Turning to the linear diblock case, it is obvious that the micelles are much more stable; the cmt lies between 45 and 52 °C (Figure 5) for the concentration range studied. Additionally, it can be seen that the concentration of the solution and the heating rate influence this parameter (Figure 5). The above results also demonstrate that the architecture of the polymer plays a major role in its micellization behavior.

The existence of a critical micelle temperature in the range of 25−60 °C for samples 8-80/50 and 600/50 gives the opportunity to study the kinetics of micelle formation, at least qualitatively. The protocol that was used for the above study involved a first heating of the solution in the light scattering cell, at about 60 °C for

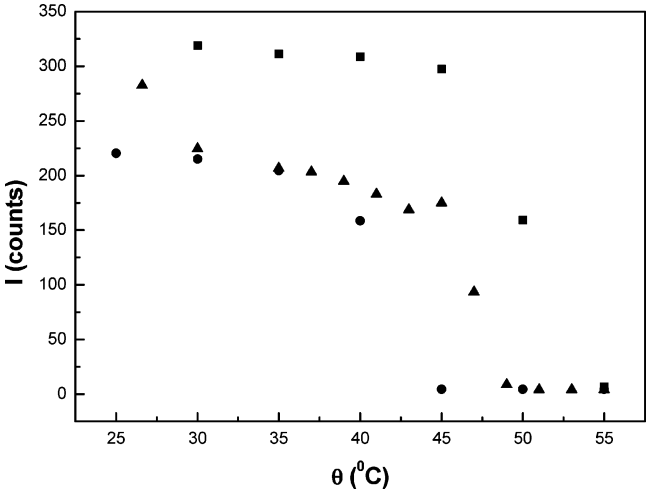

Figure 5. Light scattering intensity vs temperature, in EA, for sample 600/50: 1×10^{-3} g/mL (■), 1×10^{-4} g/mL slow heating (▲), 1×10^{-4} g/mL fast heating (●).

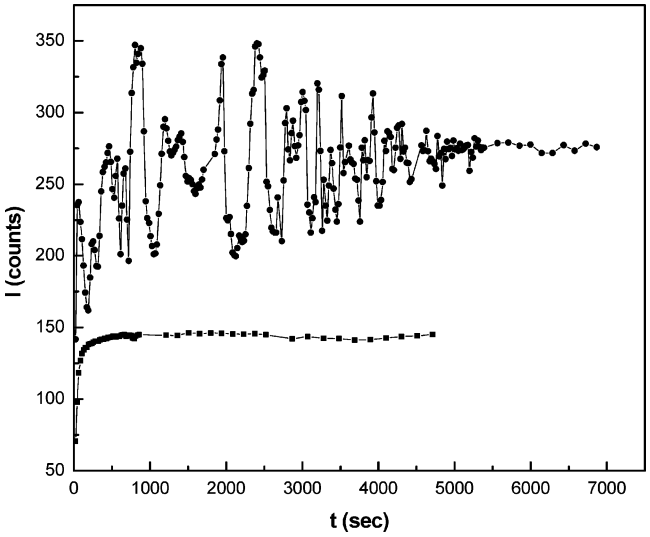

Figure 6. Time-dependent light scattering intensity, in EA, for samples 8-80/50 (■) ($c = 1 \times 10^{-2}$ g/mL) and 600/50 (●) ($c = 1 \times 10^{-3}$ g/mL).

at least 1 h. After this, immediate transport of the cell in the light scattering instrument bath of 30 °C takes place. The dead time, until the first measurement, is determined by the use of a chronometer. In Figure 6 is shown how the reduced scattering intensity (the solution intensity minus the scattering intensity of the solvent) changes during the experimental time, both for the star block and for the linear one. In the case of 8-80/50 the experimental results point to the formation of micelles after about 250 s, smoothly, as indicated by the leveling off of the scattering intensity. On the other hand, a significant fluctuation of the scattering intensity is observed for sample 600/50 before the final state is reached, using the same protocol as before. Thus, micelle formation, induced by lowering the solution temperature, was found to be faster in the star block copolymer case, although the star solution was quenched to a very shallow temperature, while the linear one was quenched to a temperature much lower than the cmt. Ideally, the comparison should be made at concentrations where only micelles are observed for both samples (i.e., at the "same distance" from the cmc) and for the same quench depth (i.e., at the "same distance" from the cmt). This

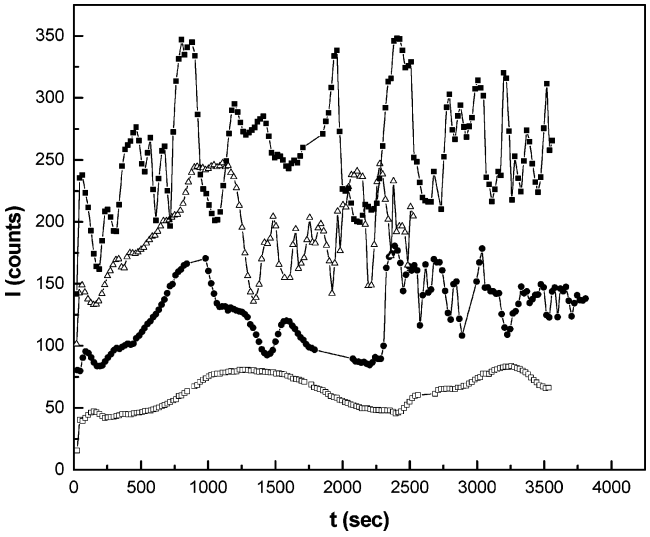

Figure 7. Light scattering intensity vs time for 600/50 in EA at different concentrations: 2×10^{-4} g/mL (□), 4×10^{-4} g/mL (●), 6×10^{-4} g/mL (△), 1×10^{-3} g/mL (■).

would ensure the same thermodynamic state for both micellar systems. In our case we tried to find the best experimental compromise for the systems at hand although a strictly ideal comparison cannot be made, since no cmc was observed for sample 600/50 and the light scattering intensities of solutions of the two polymers at the same concentration were either too high or too low. The above results indicate, in a qualitative manner, that the kinetics of 8-80/50 is much faster than that of 600/50 although the quench depth from the cmt for the star block copolymer is smaller compared to that for the diblock. The kinetics of 600/50 was further studied. In Figure 7 the changes in reduced scattering intensity for four different concentrations of this copolymer are shown. It seems that several steps in the formation of micelles exist. The fluctuations can be correlated to changes in the aggregation number of the micelles, which also seems to fluctuate until it reaches a final state. The fluctuations seem to be more dramatic as polymer concentration increases. The observed behavior has never been reported before and is completely different compared to the smooth transition for sample 8-80/50. This difference may be a result of the high molecular weight of 600/50; i.e., the core-forming block is large, and consequently, it takes a longer time to be disentangled and to be removed and inserted again into a micelle. In the case of 8-80/50 the PI part of the molecule is more compact and can move more easily as a whole. It should be mentioned that this type of time-dependent micellization is different from the previously reported anomalous micellization that concerns the formation of extraordinarily large micelles, by increasing the polymer concentration, and for concentrations close to the cmc.[44,45]

Conclusions

Differences in the micellization properties of star block copolymers, of the type $(PSPI)_8$, and linear diblock copolymers were observed, in dilute solutions in DMA and EA, by means of static and dynamic light scattering and viscometry. In the poorer for the PI block solvent, DMA, the star block copolymers were found to form micelles of smaller size, having lower aggregation number and shorter coronas compared to those of the

diblock with similar composition and molecular weight. Star block copolymers and their respective diblock arms formed micelles of essentially the same structure in DMA. In the lower selectivity solvent, EA, unimolecular micelles were formed from some diblock and star block copolymer samples. The multimolecular micelles formed by the higher molecular weight diblock and star block copolymers showed the same differences in structure as the ones observed in DMA. However, these micelles could be dissociated by an increase in temperature. Micelle formation, induced by lowering the solution temperature, was found to be faster in the star block copolymer case.

Acknowledgment. Fruitful discussions with Prof. N. Hadjichristidis are gratefully acknowledged.

Supporting Information Available: Figures S1−S4, giving scattering curves from wide-angle static light-scattering experiments and text giving a discussion thereof. This material is available free of charge via the Internet at http://pubs.acs.org.

References and Notes

(1) Tuzar, Z.; Kratochvil, P. *Surf. Colloid Sci.* **1993**, *15*, 1.
(2) Elias, H. G. *Int. J. Polym. Mater.* **1976**, *4*, 209.
(3) (a) Merrett, F. M. *J. Polym. Sci.* **1957**, *24*, 467. (b) Molau, G. E.; Wittbrodt, W. M. *Macromolecules* **1968**, *1*, 260.
(4) Honda, C.; Hasegawa, Y.; Hirunuma, R.; Nose, T. *Macromolecules* **1994**, *27*, 7660
(5) Honda, C.; Abe, Y.; Nose, T. *Macromolecules* **1996**, *29*, 6778
(6) Bednar, B.; Edwards, K.; Almgren, M.; Tormod, S.; Tuzar, Z. *Makromol. Chem., Rapid Commun.* **1988**, *9*, 785
(7) Stejskal, J.; Hlavata, D.; Sikora, A.; Konak, C.; Plestil, J.; Kratochvil, P. *Polymer* **1992**, *33*, 3675.
(8) Bahadur, P.; Sastry, N. V.; Marti, S.; Riess, G. *Colloids Surf.* **1985**, *16*, 337.
(9) Oranli, L.; Bahadur, P.; Riess, G. *Can. J. Chem.* **1985**, *63*, 2691.
(10) Antonietti, M.; Heinz, S.; Schmidt, M.; Rosenauer, C. *Macromolecules* **1994**, *27*, 3276.
(11) Forster, S.; Zisenis, M.; Wenz, E.; Antonietti, M. *J. Chem. Phys.* **1996**, *104*, 9956.
(12) Calderara, F.; Riess, G. *Macromol. Chem. Phys.* **1996**, *197*, 2115.
(13) Antonietti, M.; Forster, S.; Oestreich, S. *Macromol. Symp.* **1997**, *121*, 75.
(14) Prochazka, O.; Tuzar, Z.; Kratochvil, P. *Polymer* **1991**, *32*, 3038
(15) Balsara, N. P.; Tirrell, M.; Lodge, T. P. *Macromolecules* **1991**, *24*, 1975.
(16) Villacampa, M.; Quintana, J. R.; Salazar, R.; Katime, I. *Macromolecules* **1995**, *28*, 1025.
(17) Raspaud, E.; Lairez, D.; Adam, M.; Carton, J.-P *Macromolecules* **1994**, *27*, 2956.
(18) Tuzar, Z.; Konak, C.; Stepanek, P.; Plestil, J.; Kratochvil, P.; Prochazka, K. *Polymer* **1990**, *31*, 2118.
(19) Prochazka, K.; Glockner, G.; Hoff, M.; Tuzar, Z. *Makromol. Chem.* **1984**, *185*, 1187.
(20) Bayer, U.; Stadler, R. *Macromol. Chem. Phys.* **1994**, *195*, 2709.
(21) Iatrou, H.; Willner, L.; Hadjichristidis, N.; Halperin, A.; Richter, D. *Macromolecules* **1996**, *29*, 581.
(22) Pispas, S.; Hadjichristidis, N.; Mays, J. W. *Macromolecules* **1996**, *29*, 7378,
(23) Tsitsilianis, C.; Kouli, O. *Macromol. Rapid Commun.* **1995**, *16*, 591.
(24) Tsitsilianis, C.; Papanagopoulos, D.; Lutz, P. *Polymer* **1995**, *36*, 3745.
(25) Ramzi, A.; Prager, M.; Richter, D.; Efstratiadis, V.; Hadjichristidis, N.; Young, R. N.; Allgaier, J. B. *Macromolecules* **1997**, *30*, 7171.
(26) Pispas, S.; Poulos, Y.; Hadjichristidis, N. *Macromolecules* **1998**, *31*, 4177.
(27) Pispas, S.; Hadjichristidis, N.; Potemkin, I.; Khokhlov, A.; *Macromolecules* **2000**, *33*, 1741.
(28) Sotiriou, K.; Nannou, A.; Velis, G.; Pispas, S. *Macromolecules* **2002**, *35*, 4106.
(29) Narrainen, A. P.; Pascual, S.; Haddleton, D. M. *J. Polym. Sci., Part A: Polym. Chem.* **2002**, *40*, 439.
(30) Lele, B. S.; Leroux, J.-C. *Polymer* **2002**, *43*, 5595.
(31) Yoo, M.; Heise, A.; Hedrick, J. L.; Miller, R. D.; Frank, C. W. *Macromolecules* **2003**, *36*, 268.
(32) Heise, A.; Hedrick, J. L.; Frank, C. W.; Miller, R. D. *J. Am. Chem. Soc.* **1999**, *121*, 8647.
(33) Ishizu, K.; Uchida, S. *J. Colloid Interface Sci.* **1995**, *175*, 293.
(34) Riess, G. *Prog. Polym. Sci.* **2003**, *28*, 1107.
(35) Hadjichristidis, N.; Iatrou, H.; Pispas, S.; Pitsikalis, M. *J. Polym. Sci., Part A: Polym. Chem.* **2000**, *38*, 3211.
(36) Benoit, H.; Froelich, D. In *Light scattering from polymer solutions*; Huglin, M. B., Ed.; Academic Press: London, 1972; Chapter 11.
(37) Brandrup, J., Immergut, E. H., Eds. *Polymer Handbook*, 3rd ed.; John Wiley & Sons: New York, 1975.
(38) Batchelor, G. K. J. *Fluid Mech.* **1977**, *83*, 97.
(39) Zhang, L.; Eisenberg, A. *J. Am. Chem. Soc.* **1996**, *118*, 3168.
(40) Zhang, L.; Barlow, R. J.; Eisenberg, A. *Macromolecules* **1995**, *28*, 6055.
(41) Hadziioannou, G.; Patel, S.; Granick, S.; Tirrell, M. *J. Am. Chem. Soc.* **1986**, *108*, 2869.
(42) de Gennes, P. G. *Macromolecules* **1980**, *13*, 1069.
(43) Fetters, L. J.; Hadjichristidis, N.; Linder, J. S.; Mays, J. W. *J. Phys. Chem. Ref. Data* **1994**, *23*, 619.
(44) (a) Lally, T. P.; Price, C. *Polymer* **1974**, *15*, 325. (b) Canham, P. A.; Lally, T. P.; Price, C.; Stubberfield, R. B. *J. Chem. Soc., Faraday Trans. 1* **1980**, *76*, 1857.
(45) (a) Zhou, Z.; Chu, B. *Macromolecules* **1988**, *21*, 2548. (b) Alexandridis, P., Lindman, B., Eds. *Amphiphilic block copolymers*; Elsevier: Amsterdam, 2000; Chapter 6.

MA047937V